

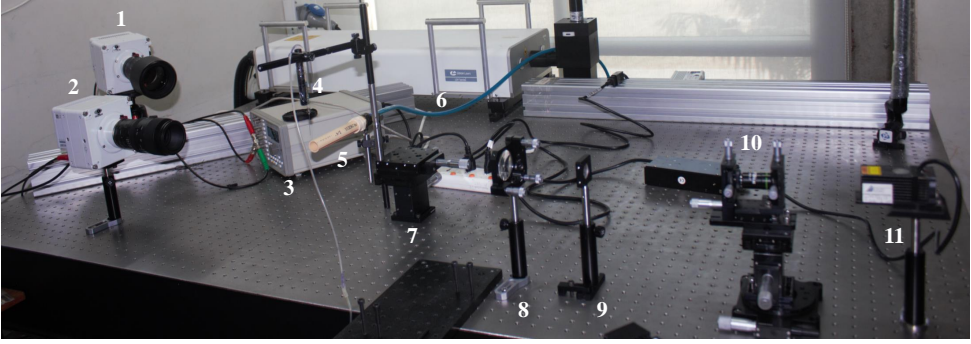
# Droplet size distribution in a swirl airstream using in-line holography technique

Someshwar Sanjay Ade,<sup>1</sup> Pavan Kumar Kirar,<sup>2</sup> Lakshmana Dora  
Chandrala<sup>3</sup> and Kirti Chandra Sahu<sup>2†</sup>

<sup>1</sup>Center for Interdisciplinary Program, Indian Institute of Technology Hyderabad, Kandi - 502  
284, Sangareddy, Telangana, India

<sup>2</sup>Department of Chemical Engineering, Indian Institute of Technology Hyderabad, Kandi - 502  
284, Sangareddy, Telangana, India

<sup>3</sup>Department of Mechanical and Aerospace Engineering, Indian Institute of Technology  
Hyderabad, Kandi - 502 284, Sangareddy, Telangana, India



(1) High-speed camera 1, (2) High-speed camera 2, (3) Synchronizer, (4) Dispensing needle, (5) Nozzle, (6) Air pipeline, (7) 3D traverser, (8) Convex lens, (9) Concave lens, (10) Spatial filter and (11) Laser.

Figure S1: A picture of our experimental set-up.

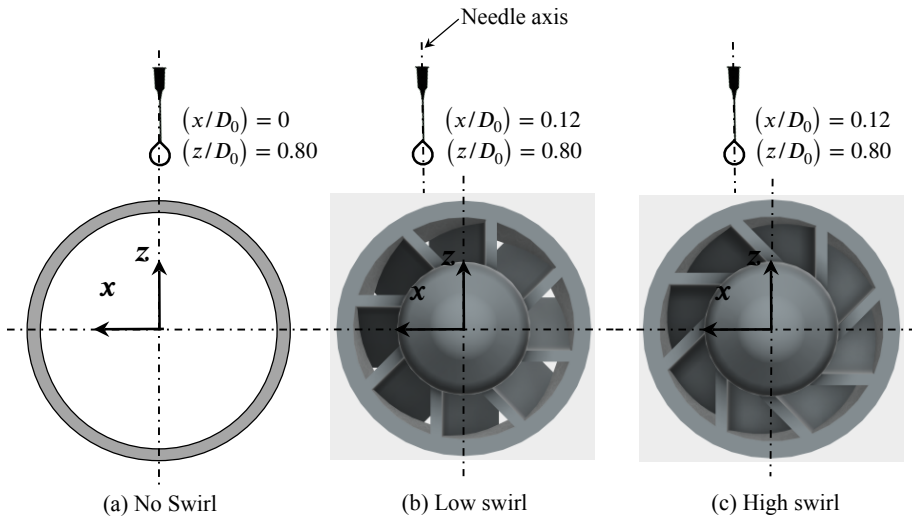


Figure S2: The dispensing needle positions for the (a) no swirl, (b) low swirl and (c) high swirl case. The images of the swirlers for the low and high swirl numbers are superimposed in panels (b) and (c), respectively.

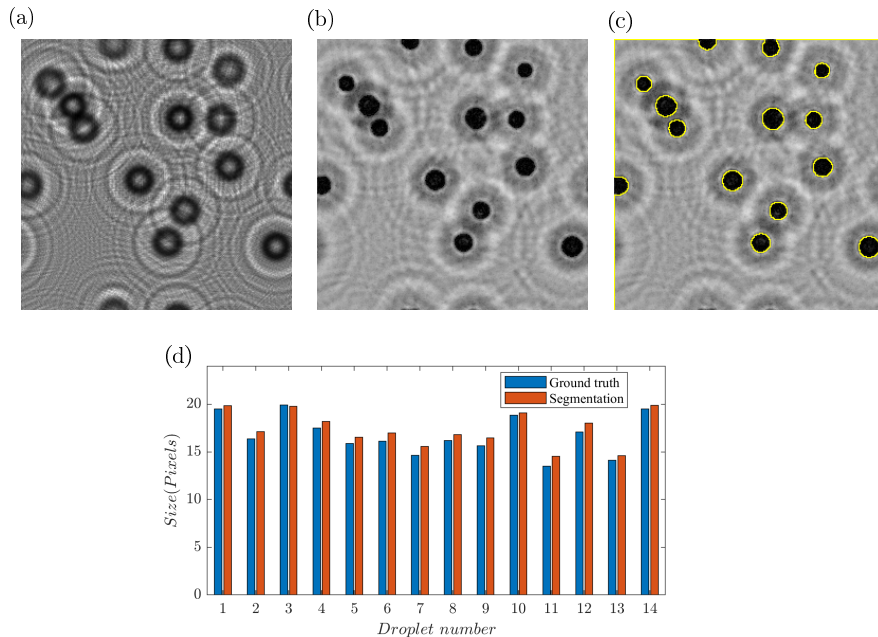


Figure S3: A demonstration of the performance of the network using synthetic data. (a) Synthetic hologram ( $256 \times 256$  pixels), (b) Minimum intensity projection after holographic reconstruction, (c) Segmentation by UNet network, and (d) A comparison of the droplet diameters between the ground truth and segmentation by Unet network.

## Network validation

In order to demonstrate the effectiveness of the network, we have created a synthetic hologram of particles following the procedure given in Gao *et al.* (2013). The synthetic hologram (Figure S3(a)) consists of 14 particles with diameters ranging from 13 to 19 pixels, which are randomly placed in a volume. The hologram is then reconstructed using the procedure described in the manuscript. In figure S3(b,c), we present the minimum intensity projection of the hologram and the segmentation of the droplets using the network. A comparison of the droplet diameters between the ground truth and segmentation by U-Net network is provided in figure S3(d). As evident from the figure S3(c,d), the network is capable of detecting all the droplets. The mean error in diameter between the ground truth and the segmented droplets by the network is about  $\pm 0.33$  pixels, which corresponds to 2 % of the mean droplet diameter.

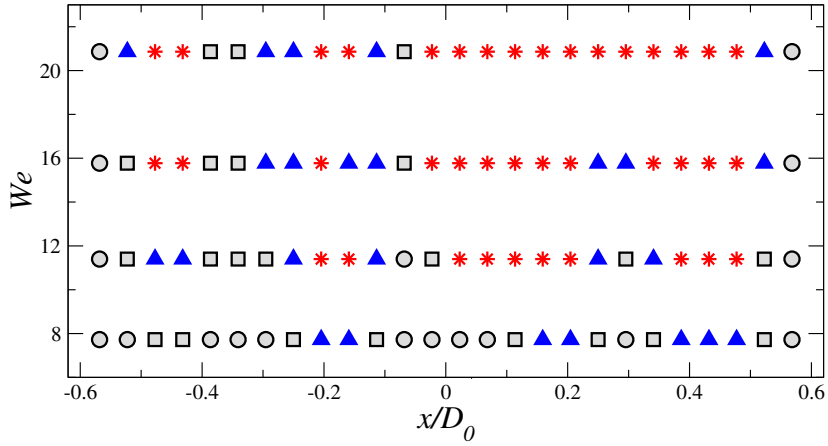


Figure S4: The regime map in  $We - x/D_0$  plane demarcating different breakup modes for  $Sw = 0.82$ . Here, circle, square, triangle and star symbols indicate no breakup, vibrational breakup, retracting bag breakup and bag breakup modes. This figure is taken from Kirar *et al.* (2022).

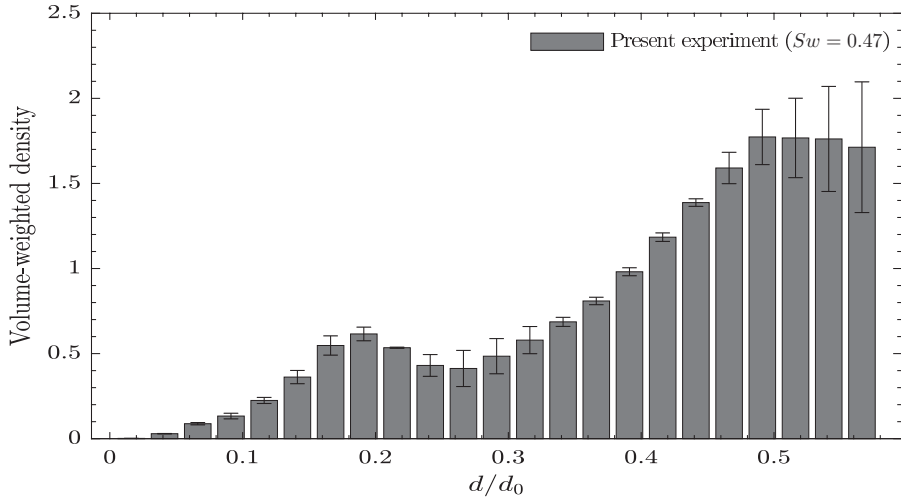


Figure S5: Volume-weighted density obtained from our experiments for  $We = 12.1$  and  $Sw = 0.47$ . The error-bar in the distribution represents the uncertainty band obtained from three experimental repetitions.

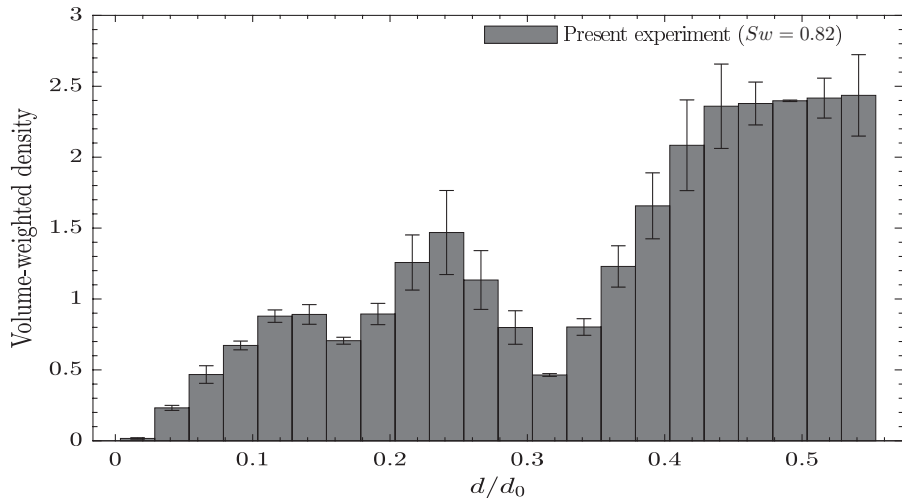


Figure S6: Volume-weighted density obtained from our experiments for  $We = 12.1$  and  $Sw = 0.82$ . The error-bar in the distribution represents the uncertainty band obtained from three experimental repetitions.

#### REFERENCES

- GAO, J., GULDENBECHER, D. R., REU, P. L. & CHEN, J. 2013 Uncertainty characterization of particle depth measurement using digital in-line holography and the hybrid method. *Optics express* **21** (22), 26432–26449.
- KIRAR, P. K., SONI, S. K., KOLHE, P. S. & SAHU, K. C. 2022 An experimental investigation of droplet morphology in swirl flow. *J. Fluid Mech.* **938**, A6.